The unique OMI HCHO/NO_2 feature during the 2008 Beijing Summer Olympics: implications for ozone production sensitivity

J. C. Witte[a,b**], B. N. Duncan[b], A. R. Douglass[b], T. P. Kurosu[c], K. Chance[c], and C. Retscher[d]

[a] Science Systems and Applications Incorporated, 10210 Greenbelt Road, Suite 600, Lanham, MD 20706, USA, ph:301-614-5991, fx:301-614-5903, email:Jacquelyn.witte@nasa.gov
[b] Atmospheric Chemistry and Dynamics Branch, NASA Goddard Space Flight Center, Greenbelt, MD 20771, USA
[c] Harvard-Smithsonian Center for Astrophysics, 60 Garden Street, Cambridge, MA 02138, USA
[d] Goddard Earth Sciences and Technology Center, University of Maryland Baltimore County, 5523 Research Park Drive, Suite 320, Baltimore, MD 21228, USA

** *Corresponding author submitted to Atmospheric Environment*

Abstract

In preparation of the Beijing Summer Olympic and Paralympics Games, strict controls were imposed between July and September 2008 on motor vehicle traffic and industrial emissions to improve air quality for the competitors. We assessed chemical sensitivity of ozone production to these controls using Ozone Monitoring Instrument (OMI) column measurements of formaldehyde (HCHO) and nitrogen dioxide (NO_2), where their ratio serves as a proxy for the sensitivity. During the emission controls, HCHO/NO_2 increased and indicated a NO_x-limited regime, in contrast to the same period in the preceding three years when the ratio indicates volatile organic carbon (VOC)-limited and mixed NO_x-VOC-limited regimes. After the emission controls were lifted, observed NO_2 and HCHO/NO_2 returned to their previous values. The 2005-2008 OMI record shows that this transition in regimes was unique as ozone production in Beijing was rarely NO_x-limited. OMI measured summertime increases in HCHO of around 13% in 2008 compared to prior years, the same time period during which MODIS vegetation indices increased. The OMI HCHO increase may be due to higher biogenic emissions of HCHO precursors, associated with Beijing's greening initiative for the Olympics. However, NO_2 and HCHO were also found to be well-correlated during the summer months. This indicates an anthropogenic VOC contribution from vehicle emissions to OMI HCHO and is a plausible explanation for the relative HCHO minimum observed in August 2008, concurrent with a minimum in traffic emissions. We calculated positive trends in 2005-2008 OMI HCHO and NO_2 of about $+1\times10^{14}$ molec cm^{-2} and $+3\times10^{13}$ molec cm^{-2} per month, respectively. The positive trend in NO_2 may be an indicator of increasing vehicular traffic since 2005, while the positive trend in HCHO may be due to a combined increase in anthropogenic and biogenic emissions since 2005.

Keywords: Air Quality, OMI, NO_2, HCHO, Beijing Olympics, Ozone abatement

1. Introduction

In 2001, Beijing, China won the bid to host the 2008 Olympics (August 8-22, 2008) and Paralympics (September 6-17, 2008) (hereafter referred to as the 'Games'), prompting health

concerns because of the city's poor air quality, which has worsened in the past several decades from rapid industrialization, population growth, and urbanization (Akimoto, 2003; Molina and Molina, 2004; Hao and Wang, 2005). Aware of Beijing's air quality issues, the Chinese government implemented aggressive short-term strategies to improve air quality during the Games between July and September 2008.

Nitrogen oxides (NO_x = NO+NO_2), volatile organic compounds (VOCs), and ozone (O_3) are among the important players in gas-phase air pollution affecting Beijing. In the presence of sunlight, NO_x and VOCs are the main ingredients for the formation of high levels of surface ozone (Haagen-Smit, 1952; Seinfeld, 1989), which has detrimental effects on human health (Hallet, 1965; Young et al., 1964; Stokinger, 1965). Photochemical oxidation of VOCs, primarily initiated by the hydroxyl radical (OH), produces organic peroxy radicals (RO_2), adding to the catalytic cycling of NO to NO_2 and the formation of ground-level ozone (Zhang et al., 2004). Oxidation of NO_2 to nitric acid and the conversion of RO_2 to peroxides break the set of chain reactions for O_3 production. Ozone production (PO_3) is nonlinearly related to concentrations of its precursors, so that ambient levels of O_3 depend on both the absolute and relative amounts of NO_x and VOC precursors (Duncan and Chameides, 1998 and references therein). Thus, strategies for controlling O_3 are to reduce emissions of either NO_x or VOCs or both (Sillman et al., 1990 and Sillman et al., 1999; Winner et al., 2000). Sillman (1995) used correlations between the afternoon concentrations of various trace gases (e.g., formaldehyde (HCHO) and total reactive nitrogen (NO_y)) to determine the chemical sensitivity of PO_3 to changes in VOCs and NO_x. Martin et al. (2004a) and Duncan et al. (2010) applied the technique of Sillman (1995) to space-based observations, demonstrating that HCHO and NO_2 from the Global Ozone Monitoring Experiment (GOME) and Ozone Monitoring Instrument (OMI) serve as reasonable proxies for *in situ* observations of VOC and NO_y in polluted environments and their ratio is a reasonable indicator of local PO_3 sensitivity.

In Beijing, PO_3 primarily is controlled by VOCs (Song et al., 2007; Wang et al. 2008; Xie et al., 2008; Chou et al., 2009), thus efforts to reduce O_3 levels should focus on VOC reduction strategies. Recent *in-situ* studies assessing the impact of emission controls on urban Beijing's air quality found that although ozone precursors decreased during the Games (Wang et al. 2009a; Wang et al., 2009b; Wang et al., 2010a), surface O_3 actually increased (Wang et al. 2010b). Wang et al. (2010b) found that surface O_3 increased 16% during the Games, despite the local pollution controls, citing regional transport of photochemically aged air and less titration of ozone by NO. Reductions in rural O_3 examined by Wang et al. (2009b) imply that the impact of the emission controls was to shift the maximum in PO_3 closer to the urban source. The local O_3 increase was an unanticipated consequence of emission reduction strategies and demonstrates the complexity of the interactions among the pollutants that affect Beijing O_3 levels.

The Games prompted the ambitious pollution control actions in and around Beijing, providing a unique opportunity to examine their effectiveness in improving ambient air quality. In this study, we use satellite data from OMI for a top-down approach to assess the impact of the controls on PO_3 during the Games. We construct 7-day running means from daily tropospheric NO_2 and total HCHO column data from OMI. We first examine changes in OMI HCHO/NO_2 [hereafter referred to as the Formaldehyde to Nitrogen Dioxide Ratio (FNR)] within the Beijing metro region (i.e., $1^\circ \times 1^\circ$ grid around the city center) during the period of emission controls (July through September 2008) and compare this FNR with other similar urban cities in China. We then address trends in HCHO and NO_2 as seen by OMI.

The satellite data are described in the following section. Section 3 outlines the emission control measures, with a focus on NO_x and VOC controls. Section 4 describes the local meteorology using rawinsondes. Section 5 discusses the effect of the emission controls on the FNR, HCHO and NO_2. We include a discussion on the growing trend we observe in OMI HCHO and NO_2 data due to increases in anthropogenic and biogenic emissions in and around Beijing. A summary follows in section 6.

2. OMI HCHO and NO_2 columns

The Ozone Monitoring Instrument (OMI), a nadir-viewing moderate resolution UV/Vis spectrometer is one of the four instruments on NASA's Aura satellite that was launched in July 2004 into a sun-synchronous orbit with an equator crossing-time of 13:38 in the ascending node, OMI has a full cross-track swath of 2600 km, containing 60 pixels ranging from 15×30 km^2 at nadir to 42×162 km^2 at the edge of the swath and provides daily global coverage, mapping pollution products on urban scales. All OMI data used in this study have been filtered to remove cloudy scenes, i.e. filtering reflectivities greater than 30%.

We use the tropospheric NO_2 columns reported as the vertical column density between the ground and the estimated mean tropopause pressure height of 150 hPa. The gridding technique of Wenig et al. (2008) weights the NO_2 vertical column densities where multiple pixels overlap and is used to produce gridded data at a horizontal resolution of $0.05^o \times 0.05^o$, smaller than the pixel size. Data were taken from the Aura Validation Data Center (AVDC) online: http://avdc.gsfc.nasa.gov. Bucsela et al. (2006) report retrieval accuracy estimates for the tropospheric column to be 25%, with a precision error of 0.25×10^{15} molec cm^{-2}.

OMI HCHO total column data are binned into $0.25^o\times0.25^o$ grids. Chance et al. (2000) showed that HCHO measurements are a very good indicator of VOCs in regions of elevated biogenic activity. Millet et al. (2006) estimated an overall error in the HCHO column data to be 25-31%. Kurosu et al. (2004) provides information on the nonlinear least-squares fitting retrieval algorithm that was originally developed for GOME and SCIAMACHY and adapted for OMI. The HCHO dataset in this study has been de-trended to remove a growing positive trend in the background values over the lifetime of OMI, i.e. a growing dark current effect in the radiance and irradiance spectra.

We calculate 7-day running means and monthly averages for HCHO and NO_2 from 2005 to 2008. Temporal averaging has been shown to reduce the HCHO measurement uncertainty and noise (Millet et al., 2008). We consider 2005-2007 in order to quantify changes in 2008 relative to previous years. We do not include 2009 results due to the growing dark current that is producing enhanced across-track striping and hot spots over ocean regions in the HCHO measurements and is too big to correct at present.

3. Emission Control Measures affecting HCHO and NO_2

We highlight relevant emission control measures (ECM) taken from a detailed summary reported by the United Nations Environment Program (UNEP) (UNEP, 2009).

NO_x was among the pollutants targeted for reduction during the Games. Streets et al. (2003) showed that a growing fraction of NO_x emissions in China is due to the rapid growth in vehicle ownership since the latter part of the 1990s. Although there are natural sources of NO_x (e.g., forest fires, lightning), the combustion of fossil fuels is the major contributor to photochemical

pollution in Eastern China (Ohara et al., 2007; Zhang et al., 2007). HCHO also contributes to the formation of photochemical pollution in urban Beijing, as an intermediate product of hydrocarbon photo-oxidation from methane, anthropogenic VOCs, and fossil fuel combustion (Pang et al., 2009; Xie et al. 2008).

From July through September 2008, stringent vehicle traffic controls were adopted, such as i) permitting entry into the city for vehicles with odd or even license plates on alternate days, and ii) banning vehicles with high emissions from entering the downtown core (UNEP report, 2009). Additional ECMs that would affect NO_x concentrations include i) reducing power plant emissions by 30% from their levels in June, well beneath the Chinese emission standard, ii) reducing output or shutting down several heavily-polluting factories, and iii) halting all construction activities (UNEP report, 2009).

Photo-oxidation of isoprene is another important source of HCHO. Isoprene (C_5H_8), the principal non-methane hydrocarbon (NMHC) emitted from vegetation (Guenther et al., 2006), is one of the most reactive NMHC, with a daytime residency of less than 1 hour against reaction with the OH radical (Trainer et al., 1987). Isoprene can contribute significantly to the total VOC reactivity in urban environments (Chameides et al., 1992). It has been shown that OMI HCHO can be used as a surrogate measure of isoprene's role in ozone formation, particularly in areas of high biogenic activity (Chance et al., 2000; Millet et al, 2008).

As part of Beijing's bid for the 2008 Games, an ambitious tree-planting program was initiated in 2001, with the goal of increasing the green coverage in the Beijing urban area by up to 40% (UNEP report, 2009). Between 2001 and 2007, UNEP reported that approximately 8,800 hectares of green space were developed using more than 30 million trees and bushes. Consequently, the vegetation cover in Beijing increased significantly over the past decade. The proportion of green space in 2006 increased by 42.5% of the total urban area compared to 2001 (Beijing Bureau of Statistics, 2007). The main species of green cover in Beijing are various broad-leaf deciduous trees, shrubbery, and lawn. Most of them are strong isoprene emitters (Zhang et al., 2000). Pang et al. (2009) and Xie et al. (2008) found that the contribution of *in situ* isoprene to local HCHO formation in Beijing is significant during the summer months and can account for 23% - 38% of the local PO_3. Yi et al. (2010) found that photo-oxidation of biogenic NMHCs, i.e,. isoprene and other alkenes, was the major source of HCHO during the Games, with HCHO contributing 22% to the total VOC measurements. Thus, the increasing vegetation coverage is expected to lead to increases of ambient isoprene and its terminal species, HCHO.

Several studies have shown that regional emissions significantly impact Beijing's air quality during the summertime when sustained southerly winds are typical (An et al., 2007; Streets et al., 2007; Wang et al., 2008). Thus, some pollution emission controls were also applied on neighboring provinces upwind of Beijing (e.g., Henan, Shanxi, and Hebei provinces located southwest and upwind of Beijing) and in the neighboring city of Tianjin, where traffic restrictions similar to Beijing's were instituted.

4. Local Weather Conditions

Regional meteorology, pollution sources and terrain all affect local air pollution in Beijing. The Taihang mountain range to the west and north of Beijing (40°N, 116°E) can trap pollution that would otherwise be exported. To the east of Beijing is the highly urban coastal city, Tianjin, and to the south are the heavily industrialized provinces of Heibei, Shanxi and Shandong. Streets

et al. (2007) found that polluted air masses from the south significantly impact Beijing's air quality during the summer months, suggesting that additional emission control measures be applied to provinces south of Beijing in preparation of the Games.

We use balloon-borne rawinsonde data launched at 12UT at the Beijing International Airport between 2005 and 2008 from the NOAA/Earth System Research Laboratory (ESRL) data archive. Rawinsondes measure the vertical distribution of temperature, RH, pressure and winds. Figure 1 shows the 7-day running mean of surface temperature, RH, wind speed and wind direction from June to September at 1000 hPa. The lines for each year are color-coded, with 2008 shown in black. The months between July and September 2005-2008 exhibit a mean temperature range from 26°C at the surface to 17°C at 850 hPa, high RH (> 50% from the surface to 850 hPa), relatively low wind speeds (2.2 m/s at the surface to 5.8 m/s at 850 hPa), and surface wind directions typically from the southwest to southeast. The prevailing southerly winds show that Beijing is located directly downwind of the heavily industrialized provinces. The mean profile of wind direction from the surface to 500 hPa is summarized in Table 1 showing winds predominantly from the south from the surface up to 850 hPa and a transition to more northerly winds from 700 hPa to 500 hPa indicating an anti-cyclonic flow that minimizes transport of boundary layer pollution into the free troposphere. Hot and humid weather prevails, creating a favorable environment for O_3 formation (Chameides and Walker, 1973; Sillman et al., 1990).

July through September 2008 exhibit typical weather patterns, although UNEP (2009) reported higher than average rainfall in Beijing during the August 2008 Olympics; such higher than average rainfall would be expected to improve air quality. Unfortunately, precipitation data are not available. However, the Beijing Meteorological Bureau showed significant improvement in air quality (e.g., NO_2) even during rain-free days, attributing these reductions to the emission controls in the city (UNEP report, 2009). Wang et al (2010b) measured NO_y and VOCs during the Games and found that while precipitation can explain some of the removal of NO_y, the VOCs were unaffected by wet removal. This lends confidence to our own analysis in which we filter for highly cloudy pixels on the assumption that these may contain precipitation events. Decreases from prior years in the remaining cloud-free data should be represent the impact of emissions reductions. Figure 1 plotted at 925 hPa and 850 hPa (not shown) also show typical summertime values for the 2005-2008 period.

5. Analysis

5.1. OMI HCHO/NO_2

Duncan et al. (2010) was the first study to use the OMI FNR to determine the PO_3 sensitivity in urban environments. Examining the Los Angeles (LA) Basin in summer, they found that FNRs < 1 indicate VOC-limited conditions, while FNRs > 2 indicate NO_x-limited conditions. FNRs between 1 and 2 represent a transition regime (i.e., a mixed VOC-NO_x-limited regime) where both NO_x and VOCs can change ozone production. For this work, we applied these regime definitions to our Beijing region since the VOC speciation determined by Song et al. (2007) and Xie et al. (2008) are similar to that of the LA Basin (Brown et al., 2007). Both cities are major metropolitan regions that experience stagnant meteorological conditions during the summer along with high traffic emissions, resulting in poor air quality.

Figure 2 shows 7-day running means of the OMI FNR, and HCHO and NO_2 columns calculated for a $1^\circ \times 1^\circ$ box around the Beijing city center (for reference, Figure 3 shows the

spatial extent of our area of interest). During the ECM, the FNRs increased above values typically observed during previous years. In general, during the summer months from 2005 to 2007, the FNRs tended towards the VOC -limited and mixed VOC-NO_x -limited regimes (highlighted in grey shading in Figure 2a). During this time period, PO_3 may have been sensitive to either VOCs and/or NO_x precursors. An exceptional period is July and August 2008, when FNRs indicated a predominantly NO_x-limited regime. This is the only period within the time series where FNR values exceeded 2 for an extended duration. We note that there were only two other episodes (mid-August 2006 and mid-July 2007) where FNR exceeded 2. During the NOx-limited period we would expect reductions in NO_x to lead to reductions in PO_3. This is supported by Wang et al. (2010b) who found that PO_3 was less sensitive to NO_x during the Olympics, compared to a previous similar study by Chou et al. (2009) which examined the August 2006 period. In September 2008, the FNRs indicated a mixed VOC-NO_x-limited regime, as compared to the more typical VOC-limited regime seen in earlier years. The peak is attributed to a combination of a minimum in NO_2 due to pollution controls (Figure 2c) and a relative peak in HCHO (Figure 2b).

Beijing is typically in a VOC-limited regime with low HCHO and high NO_2 column amounts from mid-autumn to summer (October through June) for all years. Under these conditions, PO_3 is expected to be sensitive to VOCs and respond less to changes in NO_x. This is consistent with model results reported by Fu et al. (2007). These results for northern China show increases in surface O_3 during this time period, with PO_3 being sensitive primarily to VOCs.

We repeated the analyses over a smaller $0.5^{o}\times0.5^{o}$ grid over Beijing's downtown core and the overall conclusions remain unchanged, indicating reasonable spatial homogeneity within our sampling domain. The major advantage of choosing the larger $1^{o}\times1^{o}$ grid size is that there are fewer data gaps.

5.2. Unique NO_x-Limited Case

From Figure 2a we observe a peak period between 2008/06/29 and 2008/08/15 where the FNR often exceeds 2 - well within the time period of enforced emission measures. Table 2 summarizes various statistics using data in Figure 2 during this time period of enhanced FNRs. 2008 stands out as having the highest HCHO and FNRs, as well as the lowest NO_2. In the case of NO_2, the 3.73×10^{15} molec cm^{-2} minimum in 2008 is the lowest recorded mean column amount during our study period. Table 2 shows the standard deviation and skewness of NO_2 during the peak period are also a relative minimum indicating reduced variability, relatively fewer high values, and therefore greater clustering about the mean.

We plot the spatial variability of the FNR within a $1^{o}\times1^{o}$ domain around Beijing averaged over the peak period in Figure 3. We observe that within Beijing's provincial boundaries the peak period between 2005 and 2007 reveal a dominant VOC-limited regime, with FNRs $<<1$ (darker blue contours) intensified around and slightly south of the city center (marked by the asterisk). This FNR gradually shifted to a mixed VOC-NO_x-limited regime (green) away from the city center. Here biogenic VOC sources dominate and the O_3 production is sensitive to NO_x in the photochemically aged urban plume (Duncan and Chameides, 1998). This is consistent with previous measurement studies showing that ozone production in the Beijing urban area is VOC-limited (Chou et al., 2009), while the ozone production in surrounding suburban and rural areas is NO_x-limited (Wang et al., 2006).

During the 2008 peak period, Figure 3 shows that the reductions in NO_2 due to emission controls and concomitant enhancements of FNRS occurred throughout the domain. We observe a strong NO_x-limited regime outside and well within the provincial boundaries (yellow-red). In particular, in 2008 there was a shift in FNR values in the vicinity of the city center (black box) from values less than one, typical of a VOC-limited regime, to FNR between 1 and 2 (light blue to green), indicative of a mixed VOC-NO_x regime.

The 7-day running mean of the FNR (Figure 2a) reveals instances during which the FNR exceeded 2, indicating a NO_x-limited regime. We obtain a sense of the uniqueness of these instances by comparing the FNR over Beijing during the Games to FNRs obtained for other polluted urban cities in China. We applied the same set of analyses in Figure 2 to several highly urban regions for comparison: Tianjin-Qinhuangdao, the Shanyang-Yingkou region, the Shijiazhuang to Zhenghou urban/industrial corridor, Shanghai-Nanking, and Hong Kong. We found that maximum summertime OMI FNRs never exceeded 2. Rather, these regions were in mixed VOC-NO_x-limited regimes, similar to the 2005-2007 Beijing summers, and VOC-limited regimes (< 1) during the other seasons. Figure 4 shows the July-August means per year of the FNR over China. Over these megacities (white boxes), including Beijing, we observe VOC-limited regions typical of urban environments (blue). As we move away from megacity centers the first regime shifts to mixed VOC-NO_x-limited (green), and and then to NO_x-limited region indicative of rural (or less industrial) environments (red).

5.3. HCHO and NO_2 during the ECM

High HCHO (Figure 2b) was typical from June to August for all years. We see that HCHO peaked during the summer months, in association with the seasonal maxima in surface temperatures and biogenic emissions (Fu et al., 2007). Figure 5 shows the high correlation (r^2 coefficient = 0.87) between OMI HCHO and rawinsonde surface temperatures. The Millet et al. (2008) and Duncan et al. (2010) studies showed that biogenic VOCs play a primary role in the spatial and temporal variability of OMI HCHO in the U.S., however we find evidence that anthropogenic contributions from traffic emissions impact the OMI HCHO measurements over Beijing. We use OMI NO_2 as an indicator of vehicle emissions and note that HCHO also increases with NO_2 during the summer months (Figure 6), suggesting an anthropogenic component to OMI HCHO. When we exclude the July –August 2008 control period, we calculate a positive slope of 0.07 and a reasonable correlation of 0.48. Including the control period reduces the correlation to 0.38 (dotted line), suggesting that the anthropogenic contribution to HCHO has been reduced, relative to biogenic contributions.

Figure 7 summarizes the percent changes in monthly HCHO from May to September, relative to 2008. Except for August, all the months in 2008 register increases in HCHO. The last column of Figure 7 shows an average +12% increase in May-September 2008 relative to the past three years (blue) and a +11% increase relative to 2005 (the earliest year, red). Excluding August 2008, both these increases jump to 18%. May registers the largest set of increases due to particularly low HCHO in 2006 and 2007. The minimum in August 2008 relative to prior years is interesting. Wang et al. (2010a) observed the lowest NMHC concentrations in August 2008, attributing them to a minimum in vehicle exhaust emissions. Similarly, Yi et al. (2010) measured significant reductions in vehicle emission contributions to ambient HCHO. Although we cannot discriminate the contributions of anthropogenic and biogenic sources of OMI HCHO, the

correlation with NO_2 from Figure 6 suggests that reductions in the anthropogenic component of HCHO due to vehicle emissions may explain the August 2008 minimum.

From Figure 2c, we find significant reductions in NO_2 during the ECM with a return to average values after the transportation bans were lifted at the end of September. Witte et al (2009) and Mijling (2009) gave a detailed study on OMI NO_2 during the Games. Witte et al. (2009) found an average 43% reduction in the OMI tropospheric column NO_2 between July and September 2008 compared to previous years for the same months due to traffic controls. Using a different analyses approach, Mijling et al. (2009) calculated a 59% reduction of OMI NO_2 in August 2008.

5.4. HCHO and NO_2 2005-2008 Trends

We calculate a growing trend in HCHO over Beijing using OMI data since 2005 that is consistent with increases in the biogenic emissions, i.e., Beijing's long-term initiative to expand its green cover, and anthropogenic emissions from increasing vehicular traffic (Streets et al., 2003; Zhang et al., 2007). From Table 2, we observe an increasing mean and minimum, and a reduced skewness from 2005 to 2008 indicating a shift towards higher HCHO during the peak period in FNRs. We calculate an increasing trend in HCHO of $+1\times10^{14}$ molec cm^{-2} when we remove the interannual variability by subtracting the monthly mean from the 2005-2008 monthly mean, as shown in Figure 8a. We perform the same analyses on NO_2 (Figure 8b) and, likewise, found a positive trend of $+3\times10^{13}$ molec cm^{-2} (not including the emission control period), consistent with an increasing trend in local vehicle and industrial emission sources.

We examined the 2003-2008 MODIS-Aqua 1°×1° monthly mean Normalized Difference Vegetation Index (NDVI) and Enhanced Vegetation Index (EVI) over the Beijing province to see if the increasing trend we observe in HCHO is also apparent in the vegetation indices (VIs). The VIs give a measure of 'greenness' of the Earth's land surface with increasing greenness indicating increased ground coverage by growing vegetation. The VIs complement each other in detecting vegetation changes (Huete et al., 2002). NDVI is chlorophyll sensitive with values ranging from -1 to 1. Values above 0.6 indicate dense green vegetation (Huete et al., 2002). EVI is more responsive to variations in the canopy structure, including leaf area with values greater than 0.4 indicating a high leaf area and greater canopy cover (Huete et al., 2006). These analyses were produced with the Giovanni online data system, developed and maintained by the NASA Goddard Earth Sciences Data Information Services Center (GES DISC) (Acker and Leptoukh, 2007). Table 3 summarizes the May to September monthly means using the 2003-2008 VIs. We observe that i) the peak in greenness over the Beijing region occurs in July and August, and ii) 2008 is noticeably higher compared to the 2003-2007 mean for each month suggesting enhanced vegetation. The data from Table 3 are plotted in Figure 9, similar to Figure 7. Except for the NDVI in June, all other months show persistent vegetation enhancements in 2008 relative to prior years (blue) and 2005 (red). We find NDVI and EVI increases of 3% and 7%, respectively, between the May-September 2008 mean and the 2003-2007 mean (blue). Concurrent with HCHO, in Figure 7, we also find very high VIs in May 2008, compared to other months and previous years.

Interestingly, whereas we observed a decrease in monthly HCHO in August 2008 relative to prior years (Figure 7), the VIs indicate an enhancement in vegetation. This finding is consistent with Wang et al. (2010a) who measured negligible changes in biogenic VOCs during the ECMs

364 in Beijing but calculated significant vehicle-related VOC decreases of 9-40%. This is compelling
365 evidence to suggest that OMI HCHO detected reductions in vehicle-related VOCs.
366 The positive trend in OMI HCHO and the enhancements in the VIs in 2008 relative to prior
367 years are not seen in other regions. We performed the same set of analyses shown in Figures 7
368 and 8 for Hong Kong, the Southeast US, Shanghai, and Seoul. These regions do not reveal a
369 clear positive trend or persistent VI enhancements, compared to Beijing.
370 If this increasing trend in HCHO continues it will undoubtedly affect Beijing's PO_3 sensitivity.
371 Aside from the temporary reductions gained by controlling direct emissions, further reductions
372 from natural sources will be a challenge. The pre-Games study by Chou et al. (2009) found that
373 biogenic VOCs, mostly in the form of isoprene, accounted for 22% of the PO_3 sensitivity to all
374 measured VOC species in August 2006, recommending that Beijing's ambitious tree planting
375 program consider tree species with lower isoprene emission rates as an additional means of
376 controlling ozone formation. The most recent evaluation by Wang et al (2010a) found that while
377 the ambient concentrations and PO_3 sensitivity to anthropogenic VOCs were both reduced during
378 the ECM, conversely the contributions of biogenic sources to HCHO and PO_3 sensitivity to
379 isoprene increased.
380

381 **6. Summary**

382
383 The Games in Beijing offered a real-world experiment of the effectiveness of VOC and NO_x
384 emission reductions on the chemical sensitivity of ozone formation as detected from space.
385 Duncan et al. (2010) showed that the ratio of OMI HCHO and NO_2 (i.e., the "FNR") serves as a
386 credible proxy for the ratio of VOCs and NO_x, an indicator of the sensitivity of ozone formation.
387 Following Duncan et al., we used the long-term satellite records of OMI HCHO and NO_2 to
388 show that the FNR increased in Beijing between July and September 2008 mainly as a result of
389 reduced NO_x emissions from vehicles. FNRs greater than 2 were frequently observed, indicating
390 a NO_x-limited regime where ozone formation is sensitive to changes in NO_x and not VOCs.
391 During the same period in the preceding three years, VOC-limited and mixed VOC-NO_x-limited
392 conditions were more typical, in general agreement with limitations estimated from *in situ*
393 observations reported in the literature. This change in regime indicated by OMI data is unique
394 for Beijing. We also detected higher HCHO during most of summer 2008 relative to the past
395 three years, possibly reflecting the ambitious tree planting initiatives to transform Beijing into a
396 greener city in time for the Games. The increasing trend in HCHO since 2005 is consistent with
397 increasing trends in vehicular traffic and biogenic emissions from augmented vegetation cover in
398 and around the city. A decrease in OMI HCHO in August 2008 appears to be consistent with a
399 minimum in traffic emissions. The increasing trend in NO_2 from 2005 to 2008 likely reflects the
400 known increase in vehicular traffic and industrial growth.

401

402 *Acknowledgements*: This work is supported by NASA's Atmospheric Chemistry, Modeling and
403 Analysis and Applied Sciences Air Quality Programs.
404

405 **References**

406 Acker and Leptoukh, 2007. J. G. Acker and G. Leptoukh, Online Analysis Enhances Use of
407 NASA Earth Science Data, *Eos Trans.* **88** (2007), pp. 14-17.

408 Akimoto, 2003. H. Akimoto, Global air quality and pollution. *Science* **302** (2003), pp. 1716–
409 1719, doi:10.1126/science.1092666.
410 An et al. 2007. X. An, T. Zhu Z. Wang, C. Li, and Y. Wang, A modeling analysis of a heavy air
411 pollution episode occurred in Beijing, *Atmos. Chem. Phys.* **7** (2007), pp. 3103–3114.
412 Beijing Bureau of Statistics, 2007. Beijing Bureau of Statistics, Beijing Statistics Yearbook
413 2007, China Statistics Press, Beijing (2007) (in Chinese).
414 Bucsela et al., 2006. E. Bucsela, E. Celarier, M. Wenig, J. Gleason, P. Veefkind, K.F. Boersma,
415 and E. Brinksma, Algorithm for NO_2 vertical column retrieval from the Ozone Monitoring
416 Instrument, *IEEE Transactions on Geoscience and Remote Sensing* **44** (2006), pp. 1245-
417 1258.
418 Biesenthal et al., 1997. T. Biesenthal, Q. Wu, P. Shepson, H. Wiebe, K. Anlauf, and G. Mackay,
419 A study of relationships between isoprene, its oxidation products, and ozone, in the lower
420 Fraser Valley, BC, *Atmospheric Environment* **31** (1997), pp. 2049 – 2058.
421 Brown et al., 2007. S. G. Brown, A. Frankel, and H. R. Hafner, Source apportionment of VOCs
422 in the Los Angeles area using positive matrix factorization, *Atmospheric Environment* **41**
423 (2007), pp. 227-237.
424 Cavalcante et al., 2006. R.M., Cavalcante, C. S. Campelo, M. J. Barbosa, E. R. Silveira, T. V.
425 Carvalho, and R. F. Nascimento, Determination of carbonyl compounds in air and cancer
426 Risk assessment in an academic institute in Fortaleza, Brazil, *Atmospheric Environment* **40**
427 (2006), pp. 5701-5711.
428 Chameides et al., 1992. W. Chameides et al., Ozone Precursor Relationships in the Ambient
429 Atmosphere, *J. Geophys. Res.* **97** (1992), pp. 6037-6055.
430 Chameides and Walker, 1973. W. Chameides and J. C. G. Walker, A photochemical theory of
431 tropospheric ozone, *J. Geophys. Res.* **78** (1973), pp. 8751-8760.
432 Chance et al., 2000. K. Chance, P. I. Palmer, R. J. D. Spurr, R. V. Martin, T. P. Kurosu, and D. J.
433 Jacob, Satellite observations of formaldehyde over North America from GOME, *Geophys.*
434 *Res. Lett.* **27** (2000), pp. 3461–3464.
435 Chou et al., 2009. C. Chou, C. Tsai, C. Shiu, S. Liu and T. Zhu, Measurement of NOy during the
436 Campaign of Air Quality in Beijing (CAREBeijing-2006): implications for the ozone
437 production efficiency of NOx, *J. of Geophys. Res.* **114** (2009), p. D00G01,
438 doi:10.1029/2008JD010446.
439 Duncan et al., 2010. B. N. Duncan et al., Application of OMI observations to a space-based in
440 indicator of NO_x and VOC controls on surface ozone formation, *Atmospheric Environment*
441 **44** (2010), pp. 2213-2223.
442 Duncan and Chameides, 1998. B. N. Duncan and W. L. Chameides, Effects of urban emission
443 control strategies on the export of ozone and ozone precursors from the urban atmosphere
444 to the troposphere, *J. of Geophys. Res.* **103**(D21), pp. 28159-28179.
445 Fehsenfeld et al., 1992. F. Fehsenfeld et al., Emissions of Volatile Organic Compounds From
446 Vegetation and the Implications For Atmospheric Chemistry, *Global Biogeochemical*
447 *Cycles* **6**(4), pp. 389–430.
448 Feng, Y., et al., 2005. Y. Feng, S. Wen, Y. Chen, X. Wang, H. Lü, X. Bi, G. Sheng, and J. Fu,
449 Ambient levels of carbonyl compounds and their sources in Guangzhou, China.
450 *Atmospheric Environment* **39** (2005), pp. 1789-1800.
451 Fu et al., 2007. T.-M. Fu, D. J. Jacob, P. I. Palmer, K. Chance, Y. X. Wang, B. Barletta, D. R.
452 Blake, J. C. Stanton, and M. J. Pilling, Space-based formaldehyde measurements as

453 constraints on volatile organic compound emissions in east and south Asia and implications
454 for ozone, *J. Geophys. Res.* **112** (2007), p. D06312, doi:10.1029/2006JD007853.
455 Guenther et al. 2006. A. Guenther, T. Karl, P. Harley, C. Wiedinmyer, P. I. Palmer, and C.
456 Geron, Estimates of global terrestrial isoprene emissions using MEGAN (Model of
457 Emissions of Gases and Aerosols from Nature), *Atmospheric Chemistry and Physics* **6**
458 (2006), pp. 3181–3210.
459 Haagen-Smit, 1952. A. J. Haagen-Smit, Chemistry and Physiology of Los Angeles Smog, *Ind.*
460 *Eng. Chem.* **44** (6), pp. 1342–1346, doi:10.1021/ie50510a045.
461 Hallet (1965). W. Hallet, Effect of ozone and cigarette smoke on lung function, *Arch. Environ.*
462 *Health, 10*, 295-302, 1965.
463 Hao and Wang, 2005. J. M. Hao and L. T. Wang, Improving urban air quality in China: Beijing
464 case study, *J. Air Waste Manage. Assoc.* **55** (2005), pp. 1298 – 1305.
465 Huete et al., 2002. A. Huete, K. Didan, T. Miura, E. P. Rodriguez, X. Gao, and L. G. Ferreira,
466 Overview of the radiometric and biophysical performance of the MODIS vegetation
467 indices, *Remote Sensing of Environment*, **83** (1-2) (2002), pp. 195-213.
468 Huete et al., 2006. A. Huete, K. Didan, Y. E. Shimabukuro, P. Ratana, S. R. Saleska, L. R.
469 Hutyra, W. Yang, R. R. Nemani, and R. Myneni, Amazon rainforests green-up with
470 sunlight in dry season, *Geophys. Res. Lett.*, **33** (2006), p. L06405,
471 doi:10.1029/2005GL025583.
472 Kurosu et al., 2004. T. P. Kurosu, K. Chance, and C.E. Sioris, Preliminary results for HCHO and
473 BrO from the EOS-Aura Ozone Monitoring Instrument, Passive Optical Remote Sensing of
474 the Atmosphere and Clouds IV, Proc. of SPIE Vol. 5652, doi:10.1117/12.578606.
475 Martin et al., 2004a. R. V. Martin et al., Evaluation of GOME satellite measurements of
476 tropospheric NO and HCHO using regional data from aircraft campaigns in the
477 southeastern United States, *J. Geophys. Res.* **109** (2004a), p. D24307,
478 doi:10.1029/2004JD004869.
479 Martin, R. V., A. M. Fiore, and A. Van Donkelaar (2004b), Space-based diagnosis of surface
480 ozone sensitivity to anthropogenic emissions, Geophys. Res. Lett., 31, L06120,
481 doi:10.1029/2004GL019416.
482 Mijling et al. 2009. B. Mijling, R. J. van der A, K. F. Boersma, M. Van Roozendael, I. De
483 Smedt, I., and H. M. Kelder, Reductions of NO2 detected from space during the 2008
484 Beijing Olympic Games, *Geophys. Res. Lett.* **36** (2009), p. L13801,
485 doi:10.1029/2009GL038943.
486 Millet et al. 2008. D. B. Millet, D. J. Jacob, K. F. Boersma, T.-M. Fu, T. P. Kurosu, K. Chance,
487 C. L. Heald, and A. Guenther, Spatial distribution of isoprene emissions from North
488 America derived from formaldehyde column measurements by the OMI satellite sensor, *J.*
489 *Geophys. Res.* **113** (2008), p. D02307, doi:10.1029/2007JD008950.
490 Molina and Molina, 2004. M. J. Molina and L. T. Molina, Megacities and atmospheric pollution,
491 *Journal of the Air and Waste Management Association* **5**
492 **4** (2004), pp. 644 – 680.
493 Ohara et al., 2007. T. Ohara, H. Akimoto, J. Kurokawa, N. Horii, K. Yamaji, X. Yan, and T.
494 Hayasaka, An Asian emission inventory for the period 1980–2020, *Atmos. Chem. Phys.* **7**
495 (2007), pp. 4419-4444.
496 Pang et al., 2009. X. Pang, Y. Mun, Y. Zhang, X. Lee, and J. Yuan, Contribution of isoprene to
497 formaldehyde and ozone formation based on its oxidation products measurement in

498 Beijing, China, *Atmospheric Environment* **43** (2009), pp. 2142-2147,
499 doi:10.1016/j.atmosenv.2009.01.022.
500 Seinfeld, 1989. J. Seinfeld, Urban air pollution: State of the science, *Science* **243** (1989), pp.
501 745-752.
502 Sillman, 1999. S. Sillman, The relation between ozone, NOx and hydrocarbons in urban and
503 polluted rural environments, *Atmospheric Environment* **33** (1999), pp. 1821-1845.
504 Sillman, 1995. S. Sillman, The use of NO_y, H_2O_2, and HNO_3 as indicators for ozone-NO_x-
505 hydrocarbon sensitivity in urban locations, *J. Geophys. Res.* **100 (1995), pp.** 14,175-
506 14,188.
507 Sillman et al., 1990. S. Sillman, J. Logan, and S. Wofsy, The Sensitivity of Ozone to Nitrogen
508 Oxides and Hydrocarbons in Regional Ozone Episodes, *J. Geophys. Res.* **95** (1990), pp.
509 1837-1851.
510 Song et al., 2007. Y. Song, M. Shao, Y. Liu, S. Lu, W. Kuster, P. Goldan, and S. Xie, Source
511 apportionment of ambient volatile organic compounds in Beijing, *Environmental Science*
512 *and Technology* **41** (2007), pp. 4348–4353.
513 Stokinger, H., Ozone toxicology: A review of research and industrial experience, *Arch. Environ.*
514 *Health, 10,* 719-31, 1965.
515 Streets et al., 2007. D. G. Streets et al., Air Quality during the 2008 Beijing Olympic Games,
516 *Atmospheric Environment* **41** (2007), pp. 480-492.
517 Trainer et al., 1993. M. Trainer et al., Correlation of ozone with NO_y in photochemically aged
518 air, *J. Geophys. Res.* **98** (1993), pp. 2917–2915.
519 United Nations Environment Program (UNEP), 2009. Independent Environmental Assessment:
520 Beijing 2008 Olympic Games, *UNEP* (2009), ISBN: 978-92-807-2888-0.
521 Wang et al., 2010a. B. Wang, M. Shao, S.H. Lu, B. Yuan, Y. Zhao, M. Wang, S.Q. Zhang, and
522 D. Wu, Variation of ambient non-methane hydrocarbons in Beijing city in summer 2008,
523 *Atmos. Chem. Phys.* **10** (2010a), pp. 6087-6096.
524 Wang et al., 2010b. T. Wang et al., Air quality during the 2008 Beijing Olympics: secondary
525 pollutants and regional impact, *Atmos. Chem. Phys. Discuss.* **10** (2010b), pp. 12433–12463.
526 Wang et al., 2009a. M. Wang, T. Zhu, J. Zheng, R. Y. Zhang, S. Q. Zhang, X. X. Xie, Y. Q. Han,
527 Y. and Li, Use of a mobile laboratory to evaluate changes in on-road air pollutants during the
528 Beijing 2008 Summer Olympics, *Atmos. Chem. Phys.* **9** (2009a), pp. 8247–8263.
529 Wang et al., 2009b. Y. Wang, J. Hao, M. B. McElroy, J. W. Munger, H. Ma, D. Chen, and C. P.
530 Nielsen, Ozone air quality during the 2008 Beijing Olympics – effectiveness of emission
531 restrictions, *Atmos. Chem. Phys.* **9** (2009b), pp. 5237-5251.
532 Wang et al., 2008. Q. Wang, Z. Han, T. Wang and R. Zhang, Impacts of biogenic emissions of
533 VOC and NO_x on tropospheric ozone during summertime in eastern China, *Science of The*
534 *Total Environment* **395** (2008), pp. 41-49, doi:10.1016/j.scitotenv.2008.01.059.
535 Wang et al., 2006. T. Wang, A. Ding, J. Gao, and W. S. Wu, Strong ozone production in urban
536 plumes from Beijing, China, *Geophys. Res. Lett.*, **33** (2006), p. L21806,
537 doi:10.1029/2006GL027689.
538 Wenig et al. 2008. M. O. Wenig, A. M. Cede, E. J. Bucsela, E. A. Celarier, K. F. Boersma, J. P.
539 Veefkind, E. J. Brinksma, J. F. Gleason, and J. R. Herman, Validation of OMI tropospheric
540 NO2 column densities using direct-Sun mode Brewer measurements at NASA Goddard
541 Space Flight Center, *J. Geophys. Res.* **113**, p. D16S45, doi:10.1029/2007JD008988.

Winner and Cass, 2000. D. L. Winner and G. R. Cass, Effect of emissions control on the long-term frequency distribution of regional ozone concentrations, *Environ. Sci. Technol.* **34** (2000), pp. 2612–2617.

Witte et al., 2009. J. C. Witte, M. R. Schoeberl, A. R. Douglass, J. F. Gleason, N. A. Krotkov, J. C. Gille, K. E. Pickering, and N. Livesey, Satellite observations of changes in air quality during the 2008 Beijing Olympics and Paralympics, *Geophys. Res. Lett.* **36** (2009), doi:10.1029/2009GL039236.

Xie et al., 2008. X. Xie, M. Shao, Y. Liu, S. Lu, C. Chang, and Z. Chen, 2008. Estimate of initial isoprene contribution to ozone formation potential in Beijing, China, *Atmospheric Environment* **42** (2008), pp. 6000–6010.

Young, W., D. Shaw, and D. Bates, Effects of low concentrations of ozone on pulmonary function in man, *J. Appl. Physiol., 19*, 765-8, 1964.

Zhang et al., 2007. Q. Zhang et al., NOx emission trends for China, 1995–2004: The view from the ground and the view from space, *J. Geophys. Res.* **112** (2007), p. D22306, doi:10.1029/2007JD008684.

Zhang et al., 2000. X. Zhang, Y. Mu, W. Song and Y. Zhuang, Seasonal variations of isoprene emissions from deciduous trees, *Atmospheric Environment* **34** (2000), pp. 3027–3032.

Tables and Figures

Table 1. Mean wind direction between July and September 2008 at 12Z. The Southern quadrant includes the 90°-270° hemisphere and the Northern quadrant includes 0°-90° and 270°-360°.

Year	Surface (0.06 km)		925 hPa (0.8 km)		850 hPa (~1.5 km)		700 hPa (~ 3 km)		500 hPa (~5.7 km)	
	% South	% North	% South	% North	% South	% North	% South	% North	% South	% North
2008	75.8	14.2	85.7	13.2	61.5	36.3	36.3	54.9	40.2	54.4
2007	75.0	8.7	82.6	17.4	63.0	37.0	30.4	67.4	32.6	58.7
2006	71.7	9.8	72.8	23.9	62.0	34.8	41.3	54.4	41.3	51.1
2005	66.3	13.0	71.7	27.2	60.9	38.0	33.7	65.2	41.3	54.3

Table 2. The mean, standard deviation, skewness, maximum and minimum values of the FNR ($HCHO/NO_2$), HCHO, and NO_2 calculated during the peak period between June 29 and August 15 for 2005 through 2008. Temporal averages are calculated over a $1^\circ \times 1^\circ$ box around the Beijing city center.

		2008	2007	2006	2005
$HCHO/NO_2$	Mean	2.32	1.26	1.32	1.10
	Std. Deviation	0.69	0.27	0.34	0.22
	Skewness	1.12	1.15	1.47	1.15
	Max Value	5.09	2.19	2.59	1.71
	Min Value	1.00	0.82	0.78	0.82
		2008	2007	2006	2005
HCHO ($\times 10^{16}$ molec cm^{-2})	Mean	1.46	1.37	1.35	1.33
	Std. Deviation	0.34	0.33	0.34	0.37
	Skewness	-0.03	0.12	0.49	0.73
	Max Value	2.34	2.29	2.37	2.24

	Min Value	0.75	0.68	0.65	0.66
		2008	2007	2006	2005
NO_2 ($\times 10^{15}$ molec cm^{-2})	Mean	6.44	11.00	10.49	12.20
	Std. Deviation	0.88	2.43	2.47	2.62
	Skewness	0.17	0.34	0.72	0.73
	Max Value	7.96	16.30	19.00	18.59
	Min Value	3.73	7.75	6.68	8.81

570
571 Table 3. 2003-2008 MODIS-Aqua V005 NDVI and EVI monthly values (unitless) from May to
572 September for 2005, the mean from 2003-2007, and 2008. The area average encompasses the
573 Beijing provincial borders from 39.5N-40.5N and 115.5E-117.5E.
574

	May		June		July		August		Sept.	
	NDVI	EVI	NDVI	EVI	NDVI	EVI	NDVI	EVI	NDVI	EVI
2005	0.454	0.272	0.563	0.334	0.678	0.430	0.713	0.439	0.618	0.317
Avg. (2003-2007)	0.459	0.274	0.554	0.337	0.692	0.437	0.717	0.442	0.640	0.352
2008	0.474	0.290	0.546	0.345	0.711	0.450	0.726	0.451	0.651	0.370

575
576

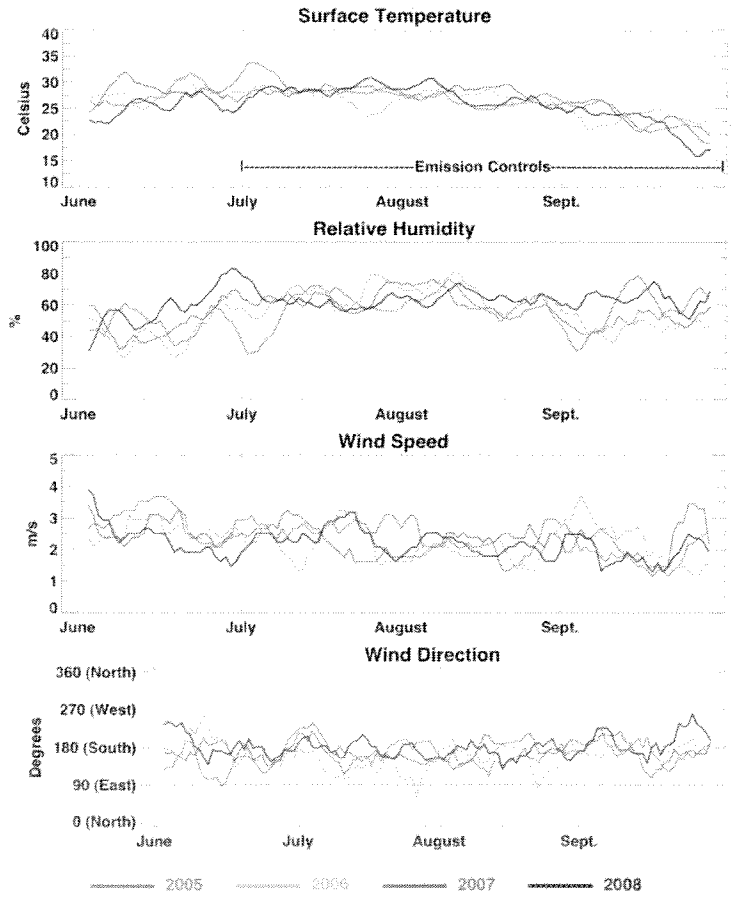

577

578
579 Figure. 1 7-day running mean of surface temperature [Celsius], relative humidity [%], wind
580 speed [m/s], and wind direction [degrees] for 2005 (blue), 2006 (green), 2007 (red), and 2008
581 (black) at 1000 hPa. Data are taken from balloon-borne rawinsondes launched daily at 12Z at the
582 Beijing International Airport (39.93°N, 116.28°E). The x-axis divides the data into its respective
583 months.
584

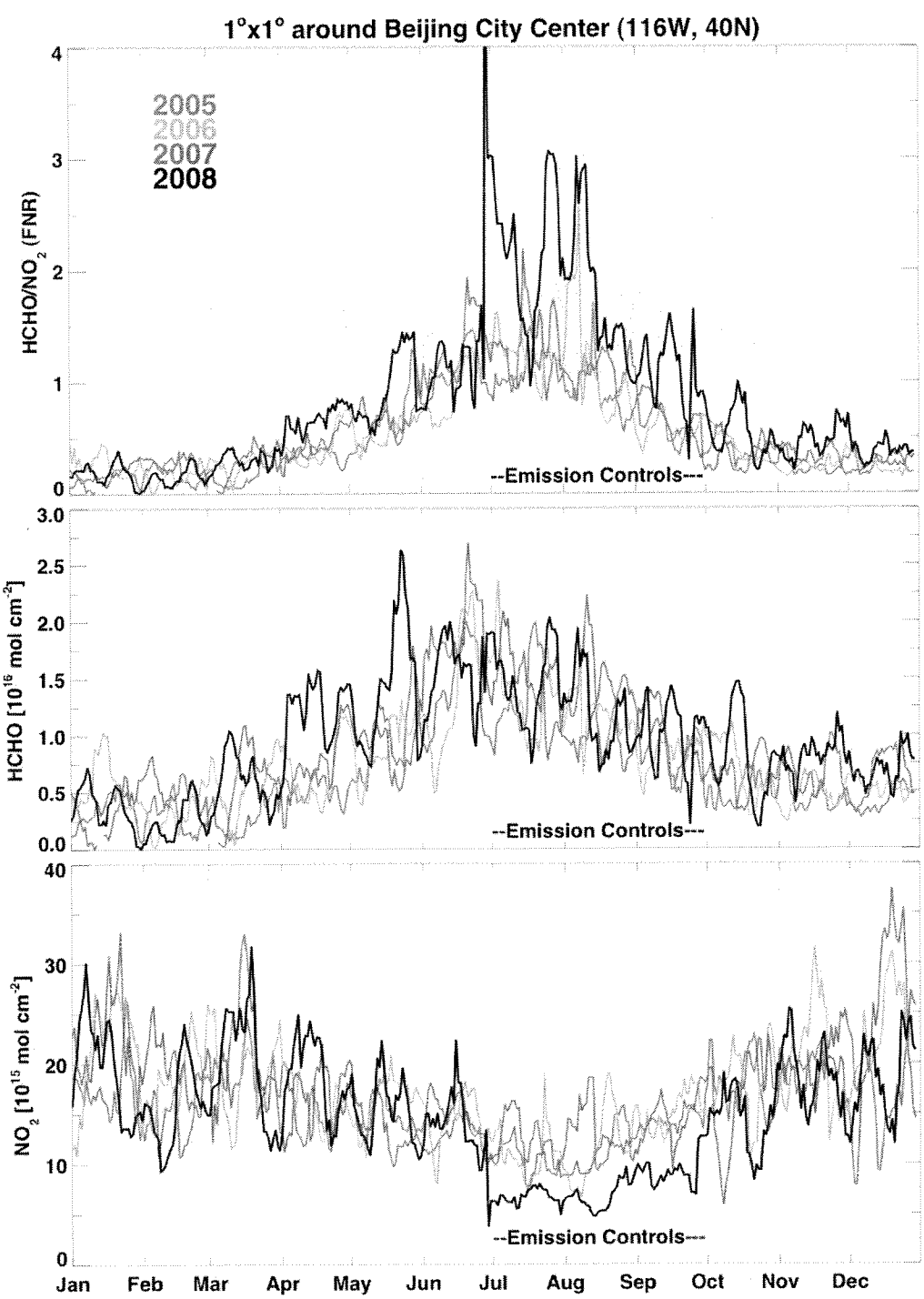

Figure 2. 7-day running means of (a) FNR, (b) HCHO total columns [10^{16} molec cm^{-2}], and (c) tropospheric NO_2 columns [10^{15} molec cm^{-2}]. The spatial average is a $1^{o}\times1^{o}$ area around the Beijing city center (39.9°N, 116.92°E) and color coded by year similar to Figure 1. The grey shading in (a) identifies the VOC-NO_x-limited regime (FNRs between 1 and 2). The time period of the strict emission controls between July and September 2008 is marked on each plot.

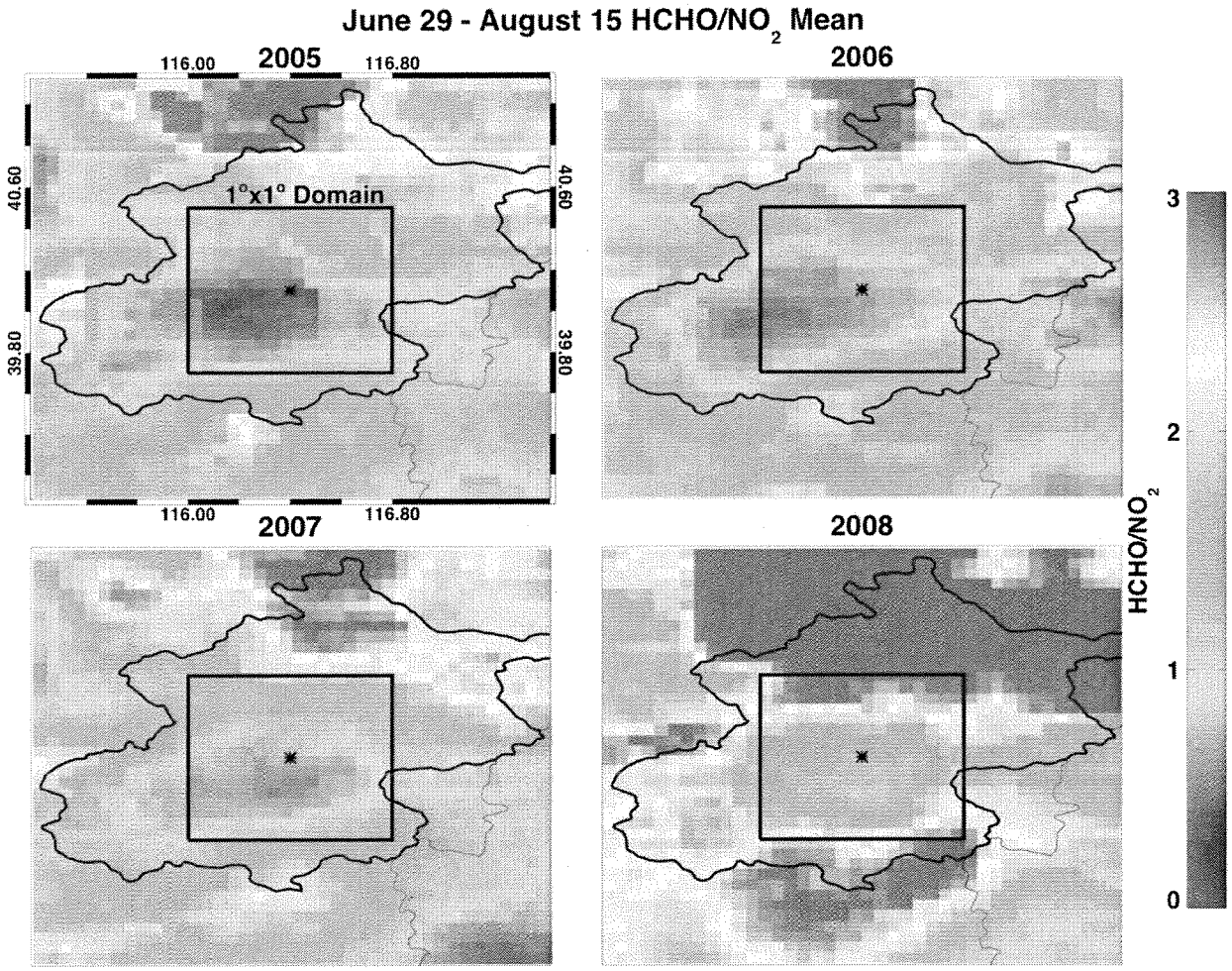

Figure 3. The FNR averaged over the June 29 to August 15 peak period for 2005 (upper left), 2006 (upper right), 2007 (lower left), and 2008 (lower right) over the Beijing province. The black box is our $1^{\circ}\times1^{\circ}$ domain around the Beijing city center, marked by an asterisk (116°E, 40°N). The thick black outline highlights the provincial boundary of Beijing.

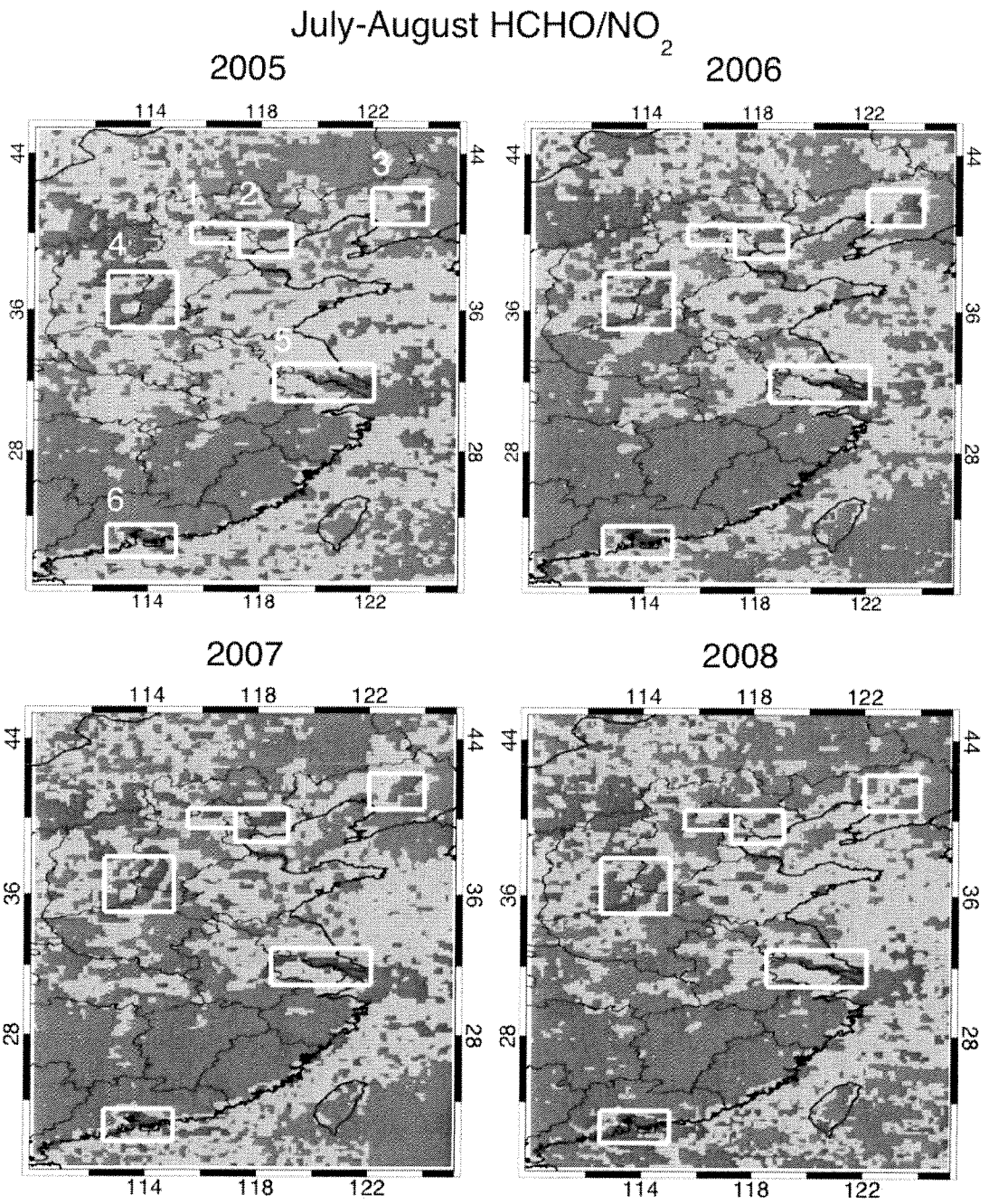

Figure 4. July-August mean of the FNRs for 2005 through 2008. The blue areas show FNRs less than 1, green indicate FNRs between 1 and 2, and red for FNRs greater than 2. Numbers in the top left panel indicate the white-boxed regions of interest: 1= Beijing province [115°N-117°N, 115°E-117°E], 2 = Tianjin-Qinhuangdao [38.5°N-41.0°N, 116.5°E-119.5°E], 3= Shanyang-Yingkou region [40.5°N-42.5°N, 122°E-125°E], 4 = Shijiazhuang to Zhenghou industrial corridor [35.0°N-38.0°N, 112.5°N-115.0°E], 5 = Shanghai-Nanking region [30.2°N-32.7°N, 118.5°E-112.5°E], and 6 = Hong Kong [21.5°N-23.5°N, 112.5°E-115°E].

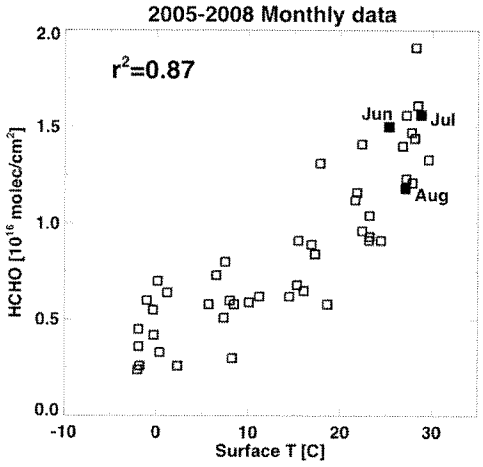

Figure 5. Monthly HCHO vs. surface temperature from the rawinsondes. The filled squares indicate the June, July, and August 2008 monthly data.

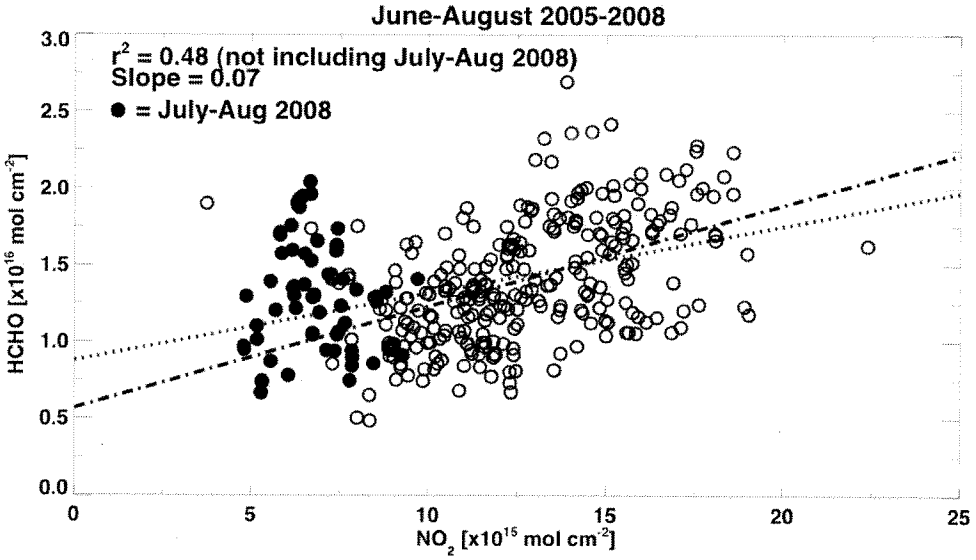

Figure 6. HCHO vs. NO_2 for June-August 2005-2008. 7-day running means are plotted over a $1^{\circ}\times1^{\circ}$ area around urban Beijing. Dash-dot line is the linear fit to the data, excluding the July-August 2008 control period. The dotted line includes the control period with an r^2 value of 0.38.

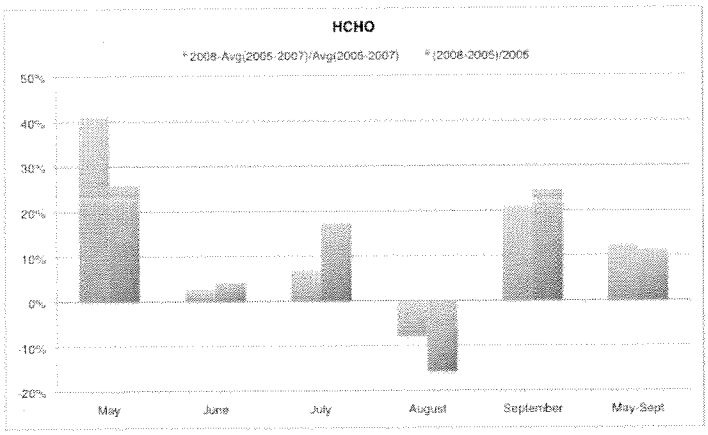

Figure 7. Monthly mean differences of HCHO from May to September, recorded as percent differences relative to 2008. The last row is the average percentage change between May and September 2008 relative to 2005.

a

b

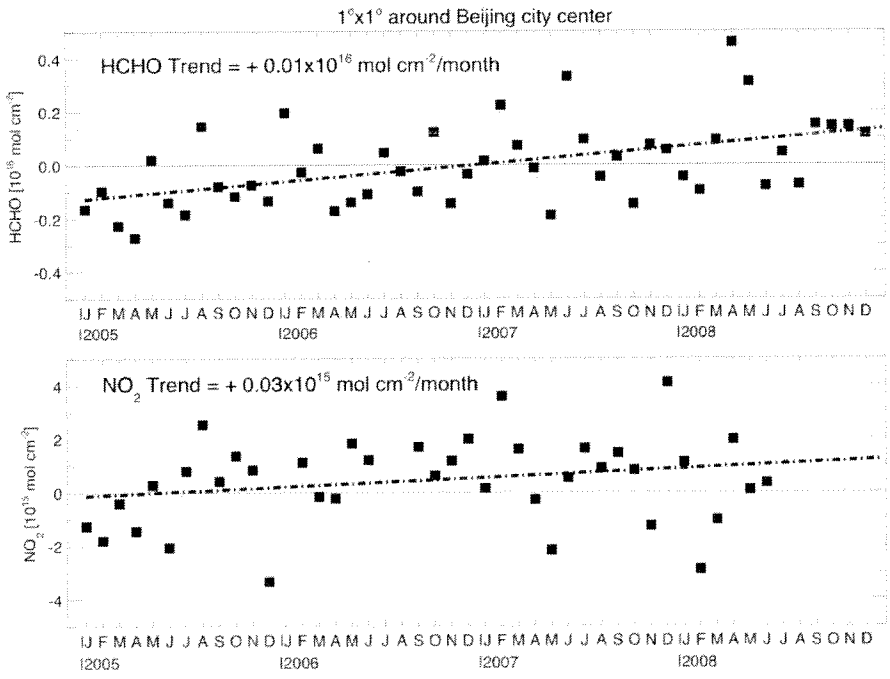

Figure 8. Monthly HCHO (a) and NO_2 (b) minus the monthly mean between 2005-2008 over a $1^{\circ}\times1^{\circ}$ area around the Beijing city center. Linear fits to the data (dashed lines) indicate small increasing trends. The NO_2 trend excludes the Olympic time period.

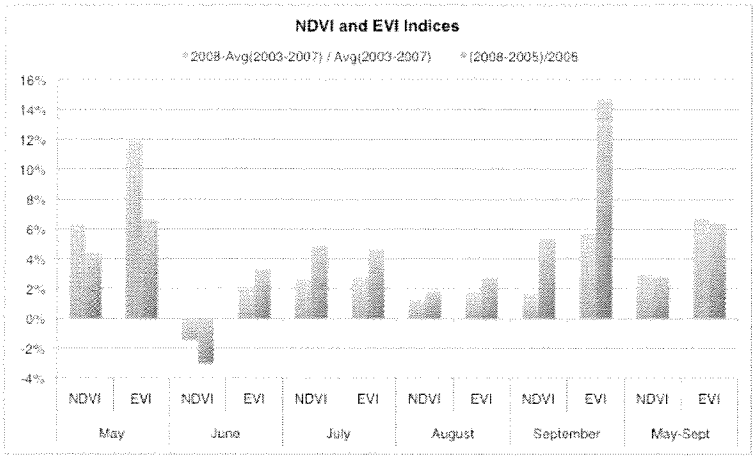

Figure 9. 2003-2008 MODIS-Aqua V005 NDVI and EVI monthly mean percentage differences relative to 2008, as in Figure 6. The area average encompasses the Beijing provincial borders from 39.5°N-40.5°N and 115.5°E-117.5°E